# A signaling axis involving CNOT3, Aurora B and ERK promotes mesendodermal differentiation of ES cells in response to FGF2 and BMP4

Moumita Sarkar[1,4], Matteo Martufi[1,4], Monica Roman-Trufero[1,4], Yi-Fang Wang[2], Chad Whilding[3], Dirk Dormann[3], Pierangela Sabbattini[1], Niall Dillon[1*].

[1] Gene Regulation and Chromatin Group, [2] Bioinformatics and Computing, [3]Microscopy Facility, MRC London Institute of Medical Sciences, Hammersmith Hospital Campus, Du Cane Road, London W12 0NN, UK.

[4]These authors contributed equally to the study

*Correspondence to niall.dillon@lms.mrc.ac.uk

**Summary**

Mesendodermal cells are key intermediate progenitors that form the early primitive streak (PrS) and give rise to mesoderm and endoderm in the gastrulating embryo. We have identified an interaction between the CCR4-NOT complex member CNOT3 and the cell cycle kinase Aurora B that regulates MAPK/ERK signalling during mesendodermal differentiation. Aurora B phosphorylates CNOT3 at two sites that are located close to a nuclear localization signal and promotes localisation of CNOT3 to the nucleus in mouse ES cells (ESCs). Mutation of these sites in ESCs gives reduced numbers of embryoid bodies that are largely composed of ectoderm and interferes with differentiation of ESCs into mesendoderm in response to FGF2, BMP4, Wnt3 and Activin. The double mutation affects interaction of CNOT3 with Aurora B and ERK leading to reduced phosphorylation of ERK in response to FGF2. Our results identify a signalling axis involving CNOT3 that regulates a key pathway during embryogenesis.

**INTRODUCTION**

A critical stage in mammalian embryogenesis is the formation of the ectoderm, mesoderm and endoderm germ layers that ultimately give rise to all of the somatic tissues in the embryo. Differentiation of the germ layers occurs during gastrulation, which begins at E6.5 in the mouse embryo with the formation of the primitive streak (PrS). The PrS starts a region of mesendodermal (ME) differentiation that forms in response to localised signalling from the hypoblast/visceral endoderm (Stern and Downs 2012). ME cells are transient precursor cells that differentiate from epiblast cells and express both mesodermal and endodermal markers (reviewed by (Wang and Chen 2016). Ingression of these cells along the midline of the primitive streak is accompanied by differentiation into mesoderm and definitive endoderm and formation of the germ layers.

A number of signalling pathways and their associated ligands have been shown to be involved in specifying the location and timing of ME differentiation and primitive streak formation in the early embryo. The ligands that signal these events include Wnt3 (Tsakiridis*, et al* 2014) together with Activin, BMP4 and FGF2 (Ben-Haim*, et al* 2006, Bernardo*, et al* 2011, Fujiwara*, et al* 2002, Tremblay*, et al* 2000). Each of these ligands has different capacities for inducing differentiation of embryonic stem cells (ESCs) into mesoderm or endoderm.  In combination they can be used to induce ESC differentiation of mesendoderm, which is characterised by expression of the mesodermal marker Brachury and endodermal markers GATA4, GATA6 and FOXA2. The fibroblast growth factor (FGF)/ERK signaling pathway plays a vital role in the formation of mesendoderm in mouse and human ESCs (Wang and Chen 2016, Yu*, et al* 2011).

3

The FGF/ERK signaling pathway functions in various embryonic developmental processes, including proliferation, survival, migration, metabolism, and differentiation (Roskoski 2012). Suppression of Erk signalling promotes ground state pluripotency in the mouse embryo and stimulated ERK activity primes lineage commitment (Kunath, *et al* 2007, Nichols, *et al* 2009). Therefore, modulation of ERK1/2 activity is critical for lineage priming and the pluripotent state of stem cells.

The CCR4-Not complex plays a key role in regulating mRNA turnover through deadenylation of polyA tails in the cytoplasm (reviewed by (Collart and Panasenko 2012). The complex is also involved in transcriptional elongation (Hu, *et al* 2009, Kruk, *et al* 2011) and in the functioning of the RNA exosome in RNA quality control and splicing in the nucleus (Collart and Panasenko 2012) (Chlebowski, *et al* 2013, Zhang, *et al* 2015). The NOT module, which is composed of Cnot1, Cnot2 and Cnot3, has been shown to have an important role in directing the catalytic module of the CCR4-Not complex to its RNA targets (Figure 1) (Boland, *et al* 2013). Cnot3 has been shown to form part of a transcriptional module in conjunction with TRIM28, c-MYC and ZFX, which binds to a number of gene promoters in ES cells (Hu, *et al* 2009). Knockout of *Cnot3* in the mouse leads to embryonic lethality at the blastocyst stage caused by loss of inner cell mass cells (Neely, *et al* 2010). Cnot3 has also been reported to inhibit differentiation of ESCs into extraembryonic lineages (Hu, *et al* 2009, Zheng, *et al* 2012).

Despite its clear importance for pluripotency, IPS cell generation and early embryonic development, analysis of the detailed roles and mechanisms of action of the CNOT3 has been complicated by its diverse functions in regulating

mRNA turnover in the cytoplasm and modulating transcription and RNA processing in the nucleus. It is also unclear how targeting of the protein to these different regulatory roles is controlled. Here we show that CNOT3 has an important role in regulating differentiation of ES cells to mesendoderm. Nuclear localisation of CNOT3 is enhanced by phosphorylation mediated by the cell cycle kinase Aurora B at two residues in CNOT3 that are located close to a consensus nuclear localisation site. We present evidence that CNOT3 interacts with Aurora B and ERK, forming part of a signalling axis that is involved in specifying mesendoderm. We also show that mutations in CNOT3 that block phosphorylation and nuclear localisation of CNOT3 reduce the level of phospho-ERK and lead to increased apoptosis of differentiating mesendoderm cells. Our results identify a novel pathway involving Cnot3, Aurora B and ERK that plays an important role in mammalian gastrulation

**RESULTS**

**Phosphorylation by Aurora B is involved in directing localisation of CNOT3 to ESC nuclei**

We initially identified Cnot3 as a potential target for the Aurora B kinase in a co-immunoprecipitation screen for proteins that bind to Aurora B in primary activated mouse B lymphocytes (Frangini, 2013) (A. Frangini and N. Dillon, unpublished data) (Figure S1A). Because of the known role of CNOT3 in pluripotency and lineage choice in ES cells, we tested whether it interacts with Aurora B in ES cells. Co-immunoprecipitation of ES cell extracts with anti-Aurora B antibody showed a strong interaction between CNOT3 and Aurora B in ES cells

5

(Figure 1A). Direct interaction of CNOT3 with Aurora B was demonstrated by *in vitro* pulldown of CNOT3 with GST-tagged Aurora B. (Figure 1B).

In vitro phosphorylation by Aurora B in the presence of $^{32}$P-ATP showed strong labelling of a Cnot3 fragment containing amino acids 275-480, indicating the presence of target sites for Aurora B phosphorylation (Figure 1C). Mass spectrometry analysis of in vitro phosphorylated CNOT3 showed that the *in vitro* phosphorylation occurs at residues T292 and S294 in the CNOT3 protein (Figure S1B). Examination of the sequence showed that the phosphorylated residues are located close to a consensus nuclear localisation sequence (NLS) (Figure 1D). This led us to consider the possibility that phosphorylation by Aurora B might affect the nuclear localisation of CNOT3. To address this question, we first transfected V5-tagged CNOT3 expression constructs carrying mutations of either T292 or S294, or of both residues, to alanine, into HEK 293 cells. The results showed reduction of nuclear CNOT3 for each of the single mutants indicating that both sites contribute to nuclear localisation in this assay (Figure S1C).

In order to directly test the role of the two residues in regulating nuclear localization of endogenous CNOT3, CRISPR/Cas9 mutagenesis was used to simultaneously mutate CNOT3-T292 and -S294 to alanine in mouse embryonic stem cells (ESCs) (Figures 1D and S1D). Generation of three ESC clones that were homozygous for the T292A/S294A double mutation was confirmed by sequencing of the mutated region (Figure S1D). The mutant ESCs grew normally and had a normal cell cycle (data not shown). Nuclear localisation of CNOT3 in the mutant ESCs was analysed by fractionation of the cells into nuclear and cytoplasmic fractions. Analysis of CNOT3 levels in the two fractions by western blotting showed a reduction in the amount of CNOT3 in the nuclei of the mutant

cells compared with wild-type cells (Figure 1E). Cytoplasmic levels of CNOT3 were largely unchanged in the mutant cells. These results provide strong evidence that phosphorylation of T292/S294 is involved in specifying localisation of CNOT3 to the ES cell nucleus.

To determine whether the effect on nuclear localisation of Cnot3 is mediated by Aurora B, wild-type ES cells were incubated for 24 and 48 hours with the specific Aurora B inhibitor AZD1152. Comparison of the levels of CNOT3 in the nuclear and cytoplasmic fractions after 24 hours incubation with AZD1152 showed a substantial reduction in the amount of CNOT3 in the nucleus (Figure 1F) and the level was further reduced after 48 hours of treatment. The level of CNOT3 in the cytoplasm was largely unaffected (Figure 1F). Propidium iodide staining and FACS analysis of the sorted cells showed only a minimal effect on the cell cycle (data not shown).

## Mutation of CNOT3-T292A/S294A affects germ layer formation in embryoid bodies

We set out to test whether the absence of phosphorylation of CNOT3-T292/S294 and the associated reduction in nuclear localization of the mutant CNOT3-DM protein affected the pluripotency and differentiation potential of the mutated ESCs. Wild-type and mutant ESCs were cultured under conditions that promoted the formation of embryoid bodies (EBs) (see Methods for details). EB formation was assessed after 4, 8 and 10 days of incubation under these conditions.  The results show that the double *Cnot3* mutation resulted in a 40% reduction in EB numbers after 10 days in culture and the average size of the EBs was reduced by 40-50% (Figure 2A and B).

7

Staining of the EBs for the lineage markers Brachyury (mesoderm), FOXA2 (Endoderm) and Nestin (Ectoderm) revealed a striking difference between the wild-type and *Cnot3*-DM EBs (Figure 2C). The EBs formed from wild-type ES cells showed strong staining for all three markers with Brachyury giving broad staining across the EB, whereas FOXA2 staining was more centrally localised. The ectodermal Nestin staining was localised to the periphery of the EBs. In contrast, the *Cnot3*-DM EBs showed very low staining for Brachyury or FOXA2 and strong staining for Nestin that was located both centrally and at the periphery of the EBs (Figure 2C). The pattern of ectodermal staining in the mutant EBs was confirmed by staining for the ectodermal marker OTX2 (Figure S2A). These results show that the mutant EBs were predominantly composed of ectoderm, which suggests that blocking phosphorylation of CNOT3-T292/S294 interferes with the differentiation of epiblast to mesendoderm that initiates germ layer formation.

**Phosphorylation of CNOT3-T292/S294 is required for efficient differentiation of ESCs into mesendoderm**

Nodal/Activin, Bmp, Wnt and FGF signaling pathways have been shown to have key roles in mesendoderm formation (Wang and Chen 2016, Yu*, et al* 2011). To further investigate the role of CNOT3-T292/S294 phosphorylation in mesendoderm differentiation, we carried out differentiations in a defined medium containing BMP4 and FGF2 and different combinations of Activin, Wnt and the GSK3b inhibitor CHIR99021 (Figure 3A-C) (see Methods). Staining for Brachyury and FOXA2 showed that all of the differentiation combinations used gave a high proportion of mesendoderm cells that stained for both markers

8

(Figure 3C). However, the numbers of differentiated mesendoderm cells obtained with the CNOT3-DM ESCs varied considerably for different ligand combinations (Figure 3B.

The most efficient differentiation of the mutant ESCs relative to wild-type (50%) was observed with the combination of Activin A, Wnt3, BMP4 and FGF2 and the biggest reduction in cell numbers for the *Cnot3*-DM mutant relative to wild-type (80%) was observed for Wnt3 + BMP4 +FGF2 (Figure 3B). Omitting Wnt3 and incubating the ESCs with BMP4 and FGF2 alone resulted in a two thirds reduction in the number of wild-type differentiated cells, but there was still a dramatic reduction (65%) in the number of surviving CNOT3-DM cells compared with the numbers obtained with wild-type ESCs. This result points to a cooperative stimulating effect of Wnt3, BMP4 and FGF2 on mesendodermal differentiation that is dependent on CNOT3 phosphorylation by Aurora B. The results also provide an explanation for the very strong effect that the T292A/S294A double mutation has on differentiation of mesoderm and endoderm in embryoid bodies.

We also tested the ability of the cells to differentiate directly into the germ layers. Wild-type and mutant ESCs were induced to differentiate into ectoderm by incubating the cells in DMEM/F12-Neurobasal medium. Differentiation into mesoderm was induced by incubating in DMEM/F12-Neurobal medium containing Activin A and differentiation into endoderm by incubation with DMEM-high glucose containing 15% FBS, FGF2 and retinoic acid. Only in the case of differentiation into endoderm induced by FGF2 and retinoic acid, did we observe reduced differentiation of the mutant cells compared with the levels observed for wild-type cells (Figure S2B). Together with the results of the mesendoderm

9

differentiations, these findings raised the possibility that CNOT3 is involved in FGF signaling.

## CNOT3-T292/S294 phosphorylation promotes survival of differentiating mesendodermal cells

Differentiation of the wild-type and mutant ESCs into mesendoderm in the presence of BMP4, and FGF2 was examined in more detail by carrying out a time-course over 8 days of differentiation (Figure 4A and 4B and Figure S3A). In addition to staining for Brachyury and FOXA2, the cells were also stained for the mesodermal marker $\alpha$-smooth muscle actin ($\alpha$-SMA) and the endodermal marker GATA4. Staining of cells that have been differentiated for 4 days is shown in Figure 4C, 4D and 4E and for 8 days in Figure S3C and S3D. The positive staining of individual cells for both these markers at the 4- and 8-day time points confirmed the identity of these cells as mesendoderm. Staining for the trophectoderm marker CDX2 gave very little staining in the differentiated cells (Figure S3E) confirming that the cells do not have the characteristics of trophectoderm. The differentiation time course clearly showed reduced numbers of the *Cnot3*-DM cells from day 2 onwards (Figure 4A and B). The observed effect on expansion of the mutant is further reinforced by the results of a time-lapse analysis of the differentiating wild-type and mutant cells between 4 and 8 days of mesendodermal differentiation (Supplementary Video 1). The time -lapse analysis showed an explosive proliferation of the wild-type cells, whereas the CNOT3-DM cells failed to expand and appeared to undergo high rates of apoptosis following cell division. Analysis of the differentiation capacity of the other two *Cnot3*-T292A/S294A mutant clones that were generated by the

10

CRISPR/CAS9 targeting showed a similar failure to expand and proliferate in the mesendoderm differentiation medium (Figure S3A), confirming that the effect was caused by the double mutation. The cell cycle profiles of the wild-type and the mutant cells after 4 days of differentiation were similar implying that the major effect of the mutation was on survival of differentiating mesendoderm cells (Figure S3B).

The susceptibility of the Cnot3-DM mutant cells to apoptosis during mesendodermal differentiation in response to FGF2 and BMP4 was directly assessed by staining wild-type and mutant cells with Annexin V and also by measuring propidium iodide (PI) uptake after 4 days of differentiation. The wild-type cells showed almost no staining for either apoptotic marker whereas the 4-day differentiated mutant cells were strongly stained for PI and Annexin V, indicating that the failure of the mutant cells to differentiate was associated with high rates of apoptosis (Figure 4F). The fact that the wild-type cells showed no sign of apoptosis whereas the mutant cells showed strong expression of an apoptotic marker suggests a functional relationship between CNOT3 phosphorylation and survival signals mediated by incubation with FGF2 and BMP4.

**The CNOT3-T292A/S294A double mutation reduces ERK phosphorylation during mesendodermal differentiation**

Erk1/2 signalling in response to stimulation by FGF is one of the major events that directs the transition from the pluripotent state to lineage commitment to the three germ layers and is critical for gastrulation (Kunath*, et al* 2007, Lanner and Rossant 2010). FGFs acts through the FGF receptors to

11

activate of the RAS/MEK ERK pathway, which culminates in phosphorylation of MAPK/ERK at the threonine and tyrosine residues of the TEY motif. Phospho-ERK is imported into the nucleus where it phosphorylates a number of transcription factors that are associated with proliferation as well as members of the RSK and MSK kinase families (Reviewed by Roux and Blenis, 2004). There is also cross-talk between Wnt signalling and the RAS/MEK/ERK pathway, with Wnt signalling upregulating ERK phosphorylation by inhibiting GSK3β and preventing it from phosphorylating and destabilising RAS (Jeong, *et al* 2018, Wang, *et al* 2006). ERK has been reported to upregulate Aurora B expression in melanoma cells (Bonet, *et al* 2012) and phosphorylated ERK plays important roles in cell survival (Mebratu and Tesfaigzi 2009).

Involvement of the FGF/MEK/ERK pathway in signalling cell survival during mesendoderm differentiation was supported by the observation that treatment of the cells with FGF and MEK inhibitors caused a dramatic reduction in cell numbers (Figure 5A). This led us to consider the possibility of a functional interaction between Aurora B, ERK and CNOT3 that would cause the CNOT3 double mutation to affect ERK phosphorylation and cell survival. Extracts from wild-type and mutant ESCs that had been differentiated with FGF2 and BMP4 for 4 days were analysed by western blotting using antibodies that recognised the phosphorylated ERK TEY motif and total ERK. The results showed a strong reduction in the level of phosphorylated ERK in the *Cnot3*-DM cells compared to wild-type (Figure 5B). Levels of phosphorylated ERK and ERK1/2 were unaffected in in undifferentiated *Cnot3*-DM ESCs (Figure S4A). Levels of CNOT3 were also reduced by differentiation of the *Cnot3*-DM cells. A similar reduction of phosphorylated ERK was observed when the differentiated cells were treated

with AZD1152, further confirming the role of Aurora B-mediated phosphorylation of CNOT3 in activating ERK (Figure 5C). A reduction in total levels of FGFR2 was also observed in the *Cnot3*-DM cells (Figure S4B) which could contribute in the reduction of phosphorylated ERK. The interaction of Aurora B and CNOT3 was further confirmed by immunoprecipitations carried out with anti-CNOT3 antibody on extracts from the 4 day differentiated cells (Figure 5D)

**Phosphorylation of CNOT3-T292/S294 regulates expression of genes that are involved in cell survival and proliferation**

To assess the changes in gene expression patterns of the mutant ESCs compared with wild-type and into mesendoderm in the presence of BMP4 and FGF2, we performed RNA sequencing (RNA-seq) analysis on the wild-type and CNOT3-DM cells after 4 days of mesendoderm differentiation (Figure 6A and 6B). The results showed 153 genes to be significantly upregulated and 155 to be downregulated in the mutant cells. Gene Ontology and GSEA analysis revealed increased expression of genes that are associated with cell death and apoptosis (Figure 6C and 6D). In addition, genes that are involved in mesenchymal, placental and epithelial cell development were upregulated (Figure 6C and 6E). These include the trophectoderm markers Cdx2 and Gata2 and the negative regulator of Wnt signalling Axin2. TGFβ, which is part of the apotosis program, was also elevated. Additionally, the Gene Ontology analysis revealed downregulation of gene expression programs that are involved in developmental processes, cell proliferation and cell signalling pathways, including the MAPK cascade (Figure 6D). The changes included downregulation of signalling

13

molecules such as FGFR2 and Wnt6. Bcl2, which is important for cell survival was also downregulated

**Phosphorylation of CNOT3-T292/S294 alters interaction of CNOT3 with Aurora B and ERK in mesendodermal cells**

To analyse interactions between Cnot3 at the single-cell level during mesendodermal differentiation, we made use of the proximity ligation assay (PLA). ESCs were incubated for 4 days in differentiation medium containing FGF2 and BMP4 and were then fixed and permeabilised and subjected to PLA using mouse anti-Aurora B and rabbit anti-Cnot3 antibodies. (see Methods). The results of this analysis (Figures 7A and S5B) showed a high level of association between CNOT3 and Aurora B in wild-type ES cells. Association foci were evenly distributed between the cytoplasm and nucleus.

Analysis of the Cnot3 mutant cells showed an unexpected increase in the interaction between CNOT3 and Aurora in the mutant cells compared to the wild-type cells after 4 days of mesendoderm differentiation (Figure 7A). The increased signal showed a similar distribution between nucleus and cytoplasm to the pattern observed in the wild type cells. Overall, these results confirm the strong interaction between CNOT3 and Aurora B that was observed by co-IP of extracts from undifferentiated ESCs and after 4 days of mesendodermal differentiation. The differences between the interaction patterns observed in the wild-type and Cnot3-T292A/S294A mutant cells suggest that phosphorylation of T292/S294 by Aurora B plays an important role in regulating the dynamic behaviour of CNOT3 in differentiating mesendoderm cells.

14

PLA was also used to analyse the interaction between CNOT3 and ERK. The results showed a substantial level of interaction in wild-type 4 day differentiated cells that was broadly distributed between cytoplasmic and nuclear compartments. The mutant cells showed significant reductions in both compartments with the cytoplasm showing a 3-fold reduction and the nuclei a 5-fold reduction in the number of interaction foci observed (Figure 7B). These results, which were confirmed with a second, separate anti-CNOT3/anti-ERK antibody pair (Figure S5A), provide strong evidence that ERK interacts with CNOT3 and that this interaction is promoted by Aurora B-mediated phosphorylation of CNOT3-T292/S294. The observation that mutation of the Aurora B phosphorylation sites reduces phosphorylation of ERK suggests that the interaction between ERK and phosphorylated CNOT3 promotes or stabilises ERK phosphorylation, thereby enhancing RAS/MEK/ERK signalling.

**DISCUSSION**

The epithelial to mesenchymal transition (EMT) that leads to mesendodermal differentiation and gastrulation is a critical stage in mammalian embryogenesis. Our results identify a role for the CNOT3 protein in regulating the signalling pathways that promote mesendodermal differentiation in the early embryo. The effect occurs through interaction between CNOT3 and the Aurora B kinase, with phosphorylation of CNOT3 by Aurora B increasing its localization to the nucleus. When the Aurora B target sites in the CNOT3 protein were mutated in ESCs, embryoid bodies formed from the mutant cells showed a dramatic reduction in differentiation of mesoderm and endoderm, with the mutant EBs being largely made up of ectoderm.

15

Differentiation of the *Cnot3*-T292A/S294A mutant ESCs into mesendoderm in response to different combinations of Activin, Wnt, BMP4 and FGF2 showed that the capacity of all four ligands to induce mesendoderm was affected by mutation of the Aurora B sites in CNOT3. The largest effect of the mutation on differentiation was observed for the combination of Wnt, BMP4 and FGF2.  This could reflect cross-talk that is known to occur between Wnt signalling and the RAS/MEK/ERK pathway (Georgopoulos*, et al* 2014, Jeong*, et al* 2018).

The observation that CNOT3 mutant cells induced to differentiate with FGF2 and BMP4 showed evidence of apoptosis whereas wild-type cells did not, suggested that CNOT3 is involved in pathways that regulate survival, with FGF2 signalling through the Ras/MEK/ERK pathway being a major candidate. This was supported by the observation that the numbers of differentiated cells obtained with wild-type cells were strongly affected by inhibition of FGF2. Analysis of ERK phosphorylation showed that ERK activation is indeed affected by the *Cnot3* mutation with a strong reduction in the levels of phosphorylated ERK observed in the mutant cells.  This finding provides a direct mechanistic explanation for the increased apoptosis observed in the *Cnot3* mutant cells when differentiation is induced using FGF2 and ERK.

How might the level of phosphorylated ERK be increased by Aurora B-mediated phosphorylation of CNOT3? Phosphorylation of ERK by MEK is followed by rapid import of phospho-ERK into the nucleus, which occurs through a variety of mechanisms (Mebratu and Tesfaigzi 2009).  Phospho-ERK is also subject to dephosphorylation in the nucleus and to re-export to the cytoplasm. The level of phospho-ERK in the nuclear compartment is known to be strongly

16

dependent on binding of ERK to stabilising proteins in the cytoplasm and in the nucleus (Caunt and McArdle 2012, Mebratu and Tesfaigzi 2009, Pouysségur and Lenormand 2003)  The results of the PLA analysis indicate that ERK interacts with CNOT3 in differentiating mesendodermal cells and that this interaction is reduced in the mutant cells by 3-fold in the cytoplasm and by 5-fold in the nucleus. Together with the observation that Aurora B phosphorylation promotes localization of CNOT3 to the nucleus, this suggests that the interaction between phosphorylated CNOT3 and ERK could be involved in stabilising phospho-ERK in the cytoplasmic and nuclear compartments and potentially in the transport of phospho-ERK into the nucleus.

The PLA analysis also revealed that mutation of the Aurora B target sites resulted in a large increase in the level of interaction between CNOT3 and Aurora B. The most likely explanation for this observation is that the interaction between Aurora B and wild-type CNOT3 is dynamic, with phosphorylation of CNOT3 leading to rapid release of the kinase from the interaction. Mutation of the phosphorylation sites would block this release by preventing phosphorylation and would lock CNOT3 into the interaction with Aurora B.

Overall, our results provide evidence of a signaling axis between ERK and Aurora B with CNOT3 acting as a key mediator between the two proteins. Our findings indicate that this axis plays an important role in regulating EMT during mesendodermal differentiation and gastrulation of the mouse embryo.

## METHODS

### Cells

E14 ESCs (female, 129/Ola) were obtained from the LMS Transgenics and ES cell facility. The ESCs were maintained on gelatin coated plates, at 37°C, 5% $CO_2$, in KnockOut Dulbecco's Modified Eagle's Medium supplemented with 15% fetal bovine serum, 1x NEAA, 2 mM L-glutamine, 100 units/ml penicillin, 100 μg/ml streptomycin, 100 μM βME (all reagents from Thermo Fisher Scientic) and 1000 units/ml LIF (Merck). HEK 293 cells (ATCC) were maintained in Dulbecco's Modified Eagle's Medium supplemented with 10% fetal bovine serum, 2 mM L-glutamine, 100 units/ml penicillin and 100 μg/ml streptomycin.

### CNOT3 gene editing using CRISPR/Cas9

The guide RNA (gRNA) used to generate the Cnot3-T292A/S294A mutant ESCs was 5'-GATTTAGACTTGGACCCACC-3'. The gRNA was cloned into pX330 (Addgene plasmid #42230) using forward primer 5'-CACCGGATTTAGACTTGGACCCACC-3' and reverse primer 5'-AAACGGTGGGTCCAAGTCTAAATCC-3'

The 110 base paired single stranded donor DNA to target Cnot3 in exon 10 carrying the mutations was: 5'-ACTCTGAAGATGATAAGAAGAGAGGCCGATCTGCGGATGCTGAAGTCAGCCAGGTGG GTCCAAGTCTAAATCTGATGGTTTGTAACTTGTTTATTGCGTGGTCTCCAAAG-3'

Mouse ESCs ($4x10^6$ cells) were transfected with 3 μg of pX330 plasmid carrying the gRNA, 4   g of the donor ssDNA and 3 μg of a puromycin resistance plasmid (pCAG-puro$^R$) using the Mouse ES Cell Nucleofector™ Kit (Lonza) following the manufacturer's protocol. One day after transfection cells were subjected to puromycin selection (1.5 μg/ml) for 24h. A week after transfection, individual

18

clones were picked and genotyped by nested PCR. Mutant genotypes were confirmed by sequencing.

**Embryoid bodies**

Half a million cells (per well of a six well plate) were seeded on ultra-low attachment plates (Corning Costar) and maintained in KnockOut Dulbecco's Modified Eagle's Medium supplemented with 15% fetal bovine serum, 1x NEAA, 2 mM L-glutamine, 100 units/ml penicillin, 100 µg/ml streptomycin, 100 µM βME and were grown up to 14 days.

Embryoid bodies (EBs) were fixed in 4% paraformaldehyde for twenty minutes followed by permeabilization with 0.5% Triton-X for twenty minutes. Subsequently, EBs were blocked in 3% BSA for one hour and then incubated with primary antibodies overnight at 4C. On the following day, the EBs were washed 3 times with PBST and incubated 1h at room temperature with the appropriate secondary antibodies. Subsequently, embryoid bodies were washed thrice in PBST and incubated with 1µg/ml DAPI in PBS for 45 minutes. Images were acquired using a Leica SP5 confocal microscope with LAS X software (Leica) and images were analysed with Fiji ImageJ software.

**Differentiation experiments**

ESC differentiation into mesendoderm: 10000 cells/cm$^2$ cells were plated on gelatin-coated plates and incubated in DMEM/F12 KnockOut media containing 64 µg/ml of L Ascorbic acid-2-phosphate magnesium, 543 µg/ml of sodium bicarbonate, 1 µg/ml of heparin, 1x insulin-transferrin-selenium, 2mM Glutamine. For the differentiations, different combinations of signalling factors were added to the medium (see "Treatments of the cells with ligands and inhibitors" below).

19

For time-lapse imaging of differentiation from day 3 to day 7, the plate was transferred to a Zeiss Axiovert 200 microscope. Phase contrast images were acquired in Leica micro-injection microscope using the MetaMorph software.

ESC differentiation to endoderm: 10000 cells/cm$^2$ cells were plated on gelatin-coated plates and incubated in high glucose DMEM with 15% FBS, 100 units/ml penicillin, 100 µg/ml streptomycin, 0.1 mM non-essential amino acids, 1mM MTG, 1x GlutaMAX and supplemented with 25 ng/ml of FGF2 and 10 µM of retinoic acid for 3 days (Kim, *et al* 2010)

ESC differentiation to mesoderm: 15000 cells/cm$^2$ were plated in gelatin + fibronectin-coated plates and incubated for 4 days in DMEM/F12-Neurobasal (1:1), N2, B27, 1x GlutaMAX, 100 units/ml penicillin, 100 µg/ml streptomycin, 0.1% β-ME and 30 ng/ml of Activin A.

ESC differentiation to ectoderm: cells were plated at a density of 15000 cells/cm$^2$ on gelatin-coated plates and incubated for 4 days in DMEM/F12-Neurobasal medium (1:1), 1x GlutaMAX, 100 units/ml penicillin, 100 µg/ml streptomycin, 100 µM βME, B27 minus Vitamin A and N2.

**Treatment of the cells with ligands and inhibitors**

Aurora B inhibitor AZD1152 (Merck)-200 nM; human recombinant Wnt3 (Cloud-Clone Corp)-200 ng/ml; Activin A (R&D Systems)-100 ng/ml; BMP4 (Merck)-10 ng/ml; FGF2 (Merck)- 25ng/ml; CHIR99021(Merck)-3µM, PD0325901 (Merck)-500nM; U0126(Merck)-10µM; AZD4547 (Abcam)-5nM.

**Cell survival assay and Annexin V staining**

The Annexin V staining was performed using the FITC Annexin V apoptosis detection kit with PI (BioLegend). Briefly, the cells were washed with PBS

followed by washing with staining buffer and resuspension in binding buffer containing Annexin V and PI and incubation for fifteen minutes at room temperature in the dark. The cells were finally washed with binding buffer and incubated with 1μg/ml DAPI in PBS for 5 minutes. Images were acquired using an Olympus IX70 microscope with Micromanager software.

Cells were stained with 0.2% crystal violet for a gross estimation of efficiency of differentiation. At different time points of differentiation live and dead cells were distinguished by trypan blue staining and counted manually. Cell survival was measured using Cell Proliferation Reagent WST-1 (Merck) following the manufacturer's instructions.

## Immunocytochemistry

All differentiated cells were grown in gelatin coated μ-slides (ibidi) for immunofluorescence. Cells were washed in PBS and fixed in 4% paraformaldehyde for ten minutes followed by permeabilization with 0.5% Triton-X for fifteen minutes. Subsequently, cells were blocked in 3% BSA for one hour and then incubated with primary antibodies overnight at 4C. After the primary antibodies the cells were washed 3 times with PBST and incubated 1h at room temperature with the appropriate secondary antibodies. Subsequently, cells were washed 3 times in PBST and incubated with 1μg/ml DAPI in PBS for 5 minutes. Images were acquired in a Leica SP5 confocal microscope with LAS X software (Leica) or Olympus IX70 microscope with Micromanager software. images were analysed with Fiji ImageJ software.

## Expression plasmids

Full length Cnot3 cDNA (Addgene) was cloned in pCDNA 3.2/V5/GW/D-TOPO by PCR addition of restriction sites SmaI/NotI following the manufacturer's

21

instructions. Cnot3-T292A, Cnot3-S294A and the double mutant was generated by site directed mutagenesis and cloned as above. An 8 μg aliquot of each DNA constructs was transfected into HEK 293 cells by Calcium Phosphate method.

**Immunoprecipitation |(IP)**

Cells were harvested in IP Lysis Buffer (50 mM Tris-HCl, pH 7.4, 150 mM NaCl, 10% glycerol, 1% Nonidet P-40, 1.0 mM EDTA) with Complete™ protease inhibitor cocktail (Merck). In all cases, 500 μg of total protein was used. The IP procedure was performed using Protein A Sepharose CL-4B beads (GE Healthcare). The extract was pre-cleared with pre-blocked beads (blocked with 1% BSA) for two hours followed by incubation with the desired primary antibodies overnight. On the following day, beads were added to it and incubated for another four hours followed by washing the beads twice with wash buffer (50 mM Tris-cl, pH 7.4, 150 mM NaCl, 10% glycerol, 0.5% Nonidet P-40, 1.0 mM EDTA). The immunocomplexes were eluted by boiling with 2x SDS loading buffer.

**Protein extractions from cells**

To obtain the whole cell extracts, cells were washed with ice cold PBS and the cell pellet was reuspended in Tris lysis buffer (50 mM Tris/HCl pH 7.5, 150 mM NaCl, 1% Triton X-100, 1 mM DTT, 1 mM $Na_3VO_4$) with Complete™ protease inhibitor cocktail (Merck).

For preparation of cytoplasmic and nuclear extracts, cells were harvested and re-suspended in harvest buffer containing 10 mM HEPES (pH 7.9), 50 mM NaCl, 0.5 M Sucrose, 0.1 mM EDTA, 0.5% Triton-X 100 and with Complete™ protease inhibitor cocktail (Merck). After obtaining the cytoplasmic extract, the nuclear pellet was further washed with wash buffer/Buffer A (10 mM HEPES (pH 7.9),

10 mM KCL, 0.1 mM EDTA and 0.1 mM EGTA), then re-suspended in Buffer C

(10 mM HEPES (pH 7.9), 500 mM NaCl, 0.1 mM EDTA, 0.1 mM EGTA, 0.1% NP40

and protease inhibitor cocktail to extract the nuclear proteins

Concentrations of the extracts were measured with the Bradford reagent (Bio-

Rad) according to the manufacturer's instructions.

## Immunoblotting

Extracts were diluted in 5x SDS loading buffer, boiled for 5 min and subjected to

SDS PAGE. Gels were transferred to nitrocellulose membranes using a Bio-Rad

wet tank blotting system. Membranes were blocked with 5% bovine serum

albumin (BSA) or 5% milk in Tris-buffered saline with 0.05% Tween-20 (TBS-T)

for 1h at room temperature and incubated with the primary antibody diluted in

2.5% BSA TBS-T O/N at 4°C. On the following day, membranes were washed 3

times for 20 min with TBS-T, incubated with the appropriate secondary antibody

(dilution 1:10000) for 1h at room temperature, washed again 3 times 15 min and

developed using Millipore Crescendo ECL (Merck) using X ray films on Photon

Imaging System or Amersham Imager 680.

## Protein purification in bacteria

Full length Aurora B cDNA (Addgene), Cnot3$_{1-102}$, Cnot3$_{275-480}$ and Cnot3$_{680-751}$

(truncations generated by PCR from full length Cnot3 cDNA (Addgene)) were

cloned into pGEX-4T1 and transformed into competent BL21 E.coli cells.

To induce protein expression, β—D-1 thiogalactopyranoside (IPTG) (Sigma) was

added at a concentration of 0.4 mM and the cells were grown for 3 hours at 37C.

The cell pellet was lysed in lysis buffer (50 mM Tris-Cl pH 8.0, 0.15 M NaCl, 1 mM

EDTA) supplemented with Complete™ protease inhibitor cocktail (Merck).

Lysozome (100 μg/ml) was added to the mix followed by addition of DTT (1 mM) and 1.5% sarcosyl followed by sonication at intervals of 15 seconds on and 45 seconds off for 5 minutes.  The clear supernatant was collected and TritonX-100 was added at a final concentration of 1% and filtered. Glutathione Sepharose High performance (GSH) beads (GE Healthcare), pre-washed in lysis buffer was added and incubated overnight at 4C. Beads were washed with washing buffer (0.5% Triton-X 100 in lysis buffer) and the GST fusion proteins were eluted with elution buffer (10mM glutathione reduced, 5% glycerol in lysis buffer) for 30 minutes at room temperature.

**GST pulldown assay**

In order to perform the GST pulldown with GST-Aurora B and Cnot3, pCDNA-Cnot3 was *in vitro* transcribed/translated using a TNT® Quick Coupled Transcription/Translation kit (Promega) according to manufacturer's instructions.  0.5 μg of the plasmid was incubated with 20 μl of TNT T7 quick Master Mix, 1 μl of [35]SMethionine 10μCi and water to a final volume of 25 μl. The reaction of transcription/translation was performed for 90 minutes at 30C. 1μg of GST or GST-Aurora B was added to GSH beads in binding buffer (50 mM Tris-cl pH 8.0, 150 mM monopotassium glutamate, 1mM EDTA, 0.1 % Igepal CAL630, 5% glycerol, 0.2% BSA) and supplemented with with Complete™ protease inhibitor cocktail (Merck), and incubated for two hours at 4C. The beads were then washed and 5 μl of the *in vitro* transcribed/translated Cnot3 was incubated with the beads overnight at 4 C. The beads were then washed with the binding buffer and the proteins were eluted by boiling in loading buffer. The eluted proteins were run on SDSPAGE, stained and dried for one hour at 80C and consequently exposed to Xray film overnight.

24

### *In vitro* kinase assay

Purified GST-CNOT3 (1 μg) fragments was incubated with 80 ng of GST-AuroraB (ProQinase) for 30 min at 30°C in phosphorylation buffer (50 mM TrisHCl pH 7.5, 10 mM $MgCl_2$, 500 μM ATP, 1 mM DTT, 5 mM NaF, 1 μl of $^{32}P\gamma$-ATP 10μCi). Reactions were stopped by addition of SDS loading buffer, boiled for 5 min and subsequently run on SDS PAGE. The gel was dried and exposed to X ray film overnight at -80C.

### Flow cytometry

Cells were trypsinised, washed twice with PBS, fixed with 70% ethanol for 30 min on ice and washed twice with 2% FBS-PBS. Subsequently, cells were resuspended in PBS containing 1μg/ml RNAse A (Thermo Fisher Scientific), 50 μg/ml propidium iodide and 0.05% NP40, incubated 20 min at room temperature in the dark followed by analysis. The experiments were performed in a LSRII (Becton-Dickinson) and analysed with FlowJo Software.

### RNA sequencing

Total RNA was extracted from $2x10^6$ cells (3 biological replicates for wild-type and CNOT3-DM cells) using Trizol reagent (Thermo Fisher Scientific) following the manufacturer's instructions. 2 μl of a 1:10 dilution of the ERCC RNA Spike-in Mix (Thermo Fisher Scientific) were added to each sample. The quality of the extracted RNA was analysed using the RNA 6000 Nano kit on a 2100 Bioanalyzer (Agilent). 500 ng of RNA was used to prepare a polyadenylated RNA library with the TruSeq Stranded mRNA Library Prep Kit (Illumina) following the manufacturer's protocol. RNA libraries were sequenced in one lane by multiplexing on an Illumina HiSeq 2500 sequencer with a 100 bp read output.

25

RNAseq reads were aligned against to Ensembl Mouse genome (NCBIM37)
reference sequence assembly and transcript annotation that obtained from Illumina
iGenomes(https://support.illumina.com/sequencing/sequencing_software/igenome.ht
ml), and to ERCC reference with Tophat2 (2.0.11) (Kim, *et al* 2013, Liao, *et al* 2014).
Gene-based read counts and ERCC counts were obtained using featureCounts
function from Rsubread Bioconductor package (Liao, *et al* 2013, Liao, *et al* 2014).
Differentially expressed gene analysis was performed with DESeq2 Bioconductor
package (Love, *et al* 2014) after normalising the data against ERCC with RUVseq
Bioconductor package (Love, *et al* 2014). Differentially expressed genes were defined
with Benjamini-Hochberg adjusted p-value<0.05 and fold change ratio > 1.5. Gene
ontology analysis was performed with goseq Bioconductor package (Young, *et al*
2010). After converting mouse gene symbol to human gene symbol using the report
of Human and Mouse Homology retrieved from Mouse Genome Informatics (MGI,
http://www.informatics.jax.org), Gene Set Enrichment Analysis (GSEA) (Mootha, *et*
*al* 2003, Subramanian, *et al* 2005) was then performed with GseaPreranked tool using
Hallmarks gene set (h.all.v5.2.symbols.gmt).

**Proximity ligation assay (PLA)**

PLA was performed using Duolink In situ Red Starter Kit Mouse/Rabbit (Merck)
following manufacturer's instructions. Briefly, cells were fixed and
permeabilised following standard conditions as described above followed by
incubation with blocking buffer (provided in the kit) for one hour at 37℃.
Subsequently, cells were incubated with desired antibodies and single antibody
controls overnight at 4℃. After the primary antibodies, the cells were washed
with wash buffers and incubated with mouse and rabbit probes for one hour at
37℃ followed by ligation reaction at 37℃ for half an hour. The amplification

reaction of the ligated product was then carried out at 37C for 90 minutes followed by counterstaining with FITC-$\alpha$Tubulin for forty minutes at room temperature. The cells were finally washed and incubated with 1$\mu$g/ml DAPI in PBS for 5 minutes. Images were acquired using a Leica SP5 confocal microscope with LAS X software (Leica). PLA dots were analysed and quantified using Imaris-Bitplane software.

## Mass spectrometry

Peptides were separated using an Ultimate 3000 RSLC nano liquid chromatography system (Thermo Fisher Scientific) coupled to an LTQ Velos Orbitrap mass spectrometer (Thermo Fisher Scientific) via a Dionex nano-esi source. Eluted peptides were analysed by the LTQ Velos operating in positive polarity using a data-dependent acquisition mode. Ions for fragmentation were determined from an initial MS1 survey scan at 60000 resolution (at m/z 200). Ion Trap CID (collisional induced dissociation), Ion Trap CID-MSA (MultiStage Activation) and HCD (Higher energy collisional induced dissociation) were carried out concurrently on the top 3 most abundant ions. For CID fragmentation methods MS1 and MS2 MSn AGC targets set to 1e6 and 1e4 for 1 microscan and a maximum injection time of 500ms and 100ms respectively. A survey scan m/z range of 350 – 1500 was used, with a normalised collision energy set to 35% for both CID and HCD, charge state rejection enabled for +1 ions and a minimum threshold for triggering fragmentation of 500 counts.

## Statistical analysis

All statistical analyses were performed with GraphPad Prism software. The statistical tests used in each experiment and significances are indicated in the corresponding figure legends.

## ACKNOWLEDGEMENTS

## REFERENCES

Ben-Haim, N., Lu, C., Guzman-Ayala, M., Pescatore, L., Mesnard, D., Bischofberger, M., Naef, F., Robertson, E.J. & Constam, D.B. (2006) The nodal precursor acting via activin receptors induces mesoderm by maintaining a source of its convertases and BMP4. *Dev Cell,* **11,** 313-323.

Bernardo, A.S., Faial, T., Gardner, L., Niakan, K.K., Ortmann, D., Senner, C.E., Callery, E.M., Trotter, M.W., Hemberger, M., Smith, J.C., Bardwell, L., Moffett, A. & Pedersen, R.A. (2011) BRACHYURY and CDX2 mediate BMP-induced differentiation of human and mouse pluripotent stem cells into embryonic and extraembryonic lineages. *Cell Stem Cell,* **9,** 144-155.

Boland, A., Chen, Y., Raisch, T., Jonas, S., Kuzuoglu-Ozturk, D., Wohlbold, L., Weichenrieder, O. & Izaurralde, E. (2013) Structure and assembly of the NOT module of the human CCR4-NOT complex. *Nat Struct Mol Biol,* **20,** 1289-1297.

Bonet, C., Giuliano, S., Ohanna, M., Bille, K., Allegra, M., Lacour, J.P., Bahadoran, P., Rocchi, S., Ballotti, R. & Bertolotto, C. (2012) Aurora B is regulated by the mitogen-activated protein kinase/extracellular signal-regulated kinase (MAPK/ERK) signaling pathway and is a valuable potential target in melanoma cells. *J Biol Chem,* **287,** 29887-29898.

Caunt, Christopher J. & McArdle, Craig A. (2012) ERK phosphorylation and nuclear accumulation: insights from single-cell imaging. *Biochem Soc Trans,* **40,** 224-229.

Chlebowski, A., Lubas, M., Jensen, T.H. & Dziembowski, A. (2013) RNA decay machines: the exosome. *Biochim Biophys Acta,* **1829,** 552-560.

Collart, M.A. & Panasenko, O.O. (2012) The Ccr4--not complex. *Gene,* **492,** 42-53.

Frangini, A. (2013) Characterization of the role of the Aurora B kinase in quiescent lymphocytes. PhD. Imperial College London.

Fujiwara, T., Dehart, D.B., Sulik, K.K. & Hogan, B.L. (2002) Distinct requirements for extra-embryonic and embryonic bone morphogenetic protein 4 in the formation of the node and primitive streak and coordination of left-right asymmetry in the mouse. *Development,* **129,** 4685-4696.

Georgopoulos, N.T., Kirkwood, L.A. & Southgate, J. (2014) A novel bidirectional positive-feedback loop between Wnt-beta-catenin and EGFR-ERK plays a role in context-specific modulation of epithelial tissue regeneration. *J Cell Sci,* **127,** 2967-2982.

Hu, G., Kim, J., Xu, Q., Leng, Y., Orkin, S.H. & Elledge, S.J. (2009) A genome-wide RNAi screen identifies a new transcriptional module required for self-renewal. *Genes Dev,* **23,** 837-848.

Jeong, W.-J., Ro, E.J. & Choi, K.-Y. (2018) Interaction between Wnt/β-catenin and RAS-ERK pathways and an anti-cancer strategy via degradations of β-catenin and RAS by targeting the Wnt/β-catenin pathway. *npj Precision Oncology,* **2,** 5.

Kim, D., Pertea, G., Trapnell, C., Pimentel, H., Kelley, R. & Salzberg, S.L. (2013) TopHat2: accurate alignment of transcriptomes in the presence of insertions, deletions and gene fusions. *Genome Biol,* **14,** R36.

Kim, J.S., Kim, B.S., Kim, J., Park, C.S. & Chung, I.Y. (2010) The phosphoinositide-3-kinase/Akt pathway mediates the transient increase in Nanog expression during differentiation of F9 cells. *Arch Pharm Res,* **33,** 1117-1125.

Kruk, J.A., Dutta, A., Fu, J., Gilmour, D.S. & Reese, J.C. (2011) The multifunctional Ccr4-Not complex directly promotes transcription elongation. *Genes Dev,* **25,** 581-593.

Kunath, T., Saba-El-Leil, M.K., Almousailleakh, M., Wray, J., Meloche, S. & Smith, A. (2007) FGF stimulation of the Erk1/2 signalling cascade triggers transition of pluripotent embryonic stem cells from self-renewal to lineage commitment. *Development,* **134,** 2895-2902.

Lanner, F. & Rossant, J. (2010) The role of FGF/Erk signaling in pluripotent cells. *Development,* **137,** 3351-3360.

Liao, Y., Smyth, G.K. & Shi, W. (2013) The Subread aligner: fast, accurate and scalable read mapping by seed-and-vote. *Nucleic Acids Res,* **41,** e108.

Liao, Y., Smyth, G.K. & Shi, W. (2014) featureCounts: an efficient general purpose program for assigning sequence reads to genomic features. *Bioinformatics,* **30,** 923-930.

Love, M.I., Huber, W. & Anders, S. (2014) Moderated estimation of fold change and dispersion for RNA-seq data with DESeq2. *Genome Biol,* **15,** 550.

Mebratu, Y. & Tesfaigzi, Y. (2009) How ERK1/2 activation controls cell proliferation and cell death: Is subcellular localization the answer? *Cell Cycle,* **8,** 1168-1175.

Mootha, V.K., Lindgren, C.M., Eriksson, K.F., Subramanian, A., Sihag, S., Lehar, J., Puigserver, P., Carlsson, E., Ridderstrale, M., Laurila, E., Houstis, N., Daly, M.J., Patterson, N., Mesirov, J.P., Golub, T.R., Tamayo, P., Spiegelman, B., Lander, E.S., Hirschhorn, J.N., Altshuler, D. & Groop, L.C. (2003) PGC-1alpha-responsive genes involved in oxidative phosphorylation are coordinately downregulated in human diabetes. *Nat Genet,* **34,** 267-273.

Neely, G.G., Kuba, K., Cammarato, A., Isobe, K., Amann, S., Zhang, L., Murata, M., Elmen, L., Gupta, V., Arora, S., Sarangi, R., Dan, D., Fujisawa, S., Usami, T., Xia, C.P., Keene, A.C., Alayari, N.N., Yamakawa, H., Elling, U., Berger, C., Novatchkova, M., Koglgruber, R., Fukuda, K., Nishina, H., Isobe, M., Pospisilik, J.A., Imai, Y., Pfeufer, A., Hicks, A.A., Pramstaller, P.P., Subramaniam, S., Kimura, A., Ocorr, K., Bodmer, R. & Penninger, J.M. (2010) A global in vivo Drosophila RNAi screen identifies NOT3 as a conserved regulator of heart function. *Cell,* **141,** 142-153.

Nichols, J., Silva, J., Roode, M. & Smith, A. (2009) Suppression of Erk signalling promotes ground state pluripotency in the mouse embryo. *Development,* **136,** 3215-3222.

Pouysségur, J. & Lenormand, P. (2003) Fidelity and spatio-temporal control in MAP kinase (ERKs) signalling. *European Journal of Biochemistry,* **270,** 3291-3299.

Roskoski, R., Jr. (2012) ERK1/2 MAP kinases: structure, function, and regulation. *Pharmacol Res,* **66,** 105-143.

Stern, C.D. & Downs, K.M. (2012) The hypoblast (visceral endoderm): an evo-devo perspective. *Development,* **139,** 1059-1069.

Subramanian, A., Tamayo, P., Mootha, V.K., Mukherjee, S., Ebert, B.L., Gillette, M.A., Paulovich, A., Pomeroy, S.L., Golub, T.R., Lander, E.S. & Mesirov, J.P. (2005) Gene set enrichment analysis: a knowledge-based approach for interpreting genome-wide expression profiles. *Proc Natl Acad Sci U S A,* **102,** 15545-15550.

Tremblay, K.D., Hoodless, P.A., Bikoff, E.K. & Robertson, E.J. (2000) Formation of the definitive endoderm in mouse is a Smad2-dependent process. *Development,* **127,** 3079-3090.

Tsakiridis, A., Huang, Y., Blin, G., Skylaki, S., Wymeersch, F., Osorno, R., Economou, C., Karagianni, E., Zhao, S., Lowell, S. & Wilson, V. (2014) Distinct Wnt-driven primitive streak-like populations reflect in vivo lineage precursors. *Development,* **141,** 1209-1221.

Wang, L. & Chen, Y.G. (2016) Signaling Control of Differentiation of Embryonic Stem Cells toward Mesendoderm. *J Mol Biol,* **428,** 1409-1422.

Wang, Q., Zhou, Y., Wang, X. & Evers, B.M. (2006) Glycogen synthase kinase-3 is a negative regulator of extracellular signal-regulated kinase. *Oncogene,* **25,** 43-50.

Young, M.D., Wakefield, M.J., Smyth, G.K. & Oshlack, A. (2010) Gene ontology analysis for RNA-seq: accounting for selection bias. *Genome Biol,* **11,** R14.

Yu, P., Pan, G., Yu, J. & Thomson, J.A. (2011) FGF2 sustains NANOG and switches the outcome of BMP4-induced human embryonic stem cell differentiation. *Cell Stem Cell,* **8,** 326-334.

Zhang, L., Wan, Y., Huang, G., Wang, D., Yu, X., Huang, G. & Guo, J. (2015) The exosome controls alternative splicing by mediating the gene expression and assembly of the spliceosome complex. *Sci Rep,* **5,** 13403.

Zheng, X., Dumitru, R., Lackford, B.L., Freudenberg, J.M., Singh, A.P., Archer, T.K., Jothi, R. & Hu, G. (2012) Cnot1, Cnot2, and Cnot3 maintain mouse and human ESC identity and inhibit extraembryonic differentiation. *Stem Cells,* **30,** 910-922.

**FIGURE LEGENDS**

**Figure 1: Phosphorylation by Aurora B is involved in directing localisation of CNOT3 to ESC nuclei. A.** Immunoprecipitation (IP) carried out on cell extracts prepared from wild-type ESCs using anti-Aurora B antibody. Blots were probed with anti-CNOT3 antibody (top) and anti-Aurora B antibody (bottom). IP with normal mouse IgG was used as a negative control. Input = 5% of the extract. **B.** *In vitro* GST pulldown assay using GST-Aurora B and *in vitro* transcribed/translated Cnot3, labelled with $^{35}$SMethionine. GST-only was used as a negative control. Input =10% labelled Cnot3. **C.** *In vitro* kinase assay using γ-$^{32}$P-ATP with purified GST-CNOT3 fragments (see numbers above lanes. Mass spectrometry data (Figure S1B) showed that CNOT3-T292 and -S294 are the sites of phosphorylation by Aurora B. **D.** Schematic representation of structure of the domains of CNOT3 and the position of the consensus nuclear localisation signal (NLS). **E.** Immunoblotting analysis of CNOT3 levels in cytoplasmic and nuclear extracts of wild-type and *Cnot3*-DM ESCs. Cytoplasmic loading control: α-Tubulin. Nuclear loading control: Histone H3. **F.** Immunoblotting analysis of CNOT3 from cytoplasmic and nuclear extracts of wild-type (WT) and *Cnot3*-DM ESCs, treated with Aurora B inhibitor AZD1152 for 24 hours and 48 hours respectively before harvesting. DMSO: vehicle control. Cytoplasmic loading control: α-Tubulin. Nuclear loading control: Lamin B.

**Figure 2: Mutation of CNOT3-T292A/S294 affects germ layer formation in embryoid bodies. A.** Representative phase-contrast images of embryoid bodies (EBs) formed from WT and *Cnot3*-DM ESCs after 4 and 10 days. Scale bar: 100 μm.

31

**B.** Histograms show the number and size (area) of EBs formed from *Cnot3*-DM ESCs relative to WT cells at 4, 8 and 10 days respectively. Mean ± SEM; *t*-test ***P<0.001 *n*=3. **C.**   Left panel: Representative confocal images of EBs derived from WT and *Cnot3*-DM ESCs stained with the mesodermal marker Brachury (*red*) and endodermal marker FOXA2 (green) at 8 days (scale bar:6 mm). Right panel: staining for ectodermal marker nestin (green) (scale bar: 100 μm). Nuclei were stained with DAPI. Staining for an additional ectodermal marker OTX2 is shown in Figure S2A.

**Figure 3: Phosphorylation of CNOT3-T292/S294 is required for efficient differentiation of ESCs into mesendoderm. A.** Representative phase-contrast images showing the efficiency of mesendoderm differentiation of WT and *Cnot3*-DM ESCs over 4 days in the presence of various combinations (as indicated) of Activin A, CHIR99021, Wnt3 and BMP4 + FGF2. Scale bar: 100 μm.  **B.** Histogram shows the survival of WT and *Cnot3*-DM ESCs treated with different combinations of the ligands used in A over 4 days of mesendoderm differentiation. Activin A, CHIR99021 and Wnt3 was added after two days of BMP4+FGF2 induced differentiation and the cell survival was determined using WST-1 reagent on day 4 of the differentiation. Survival ratios were calculated relative to the values obtained for WT cells treated with Activin A+ BMP4+FGF2. Mean ± SEM; Significance was calculated between WT and CNOT3-DM for each combination using unpaired *t*-test ***P<0.001 *n*=3.  **C.** Representative IF images of mesodermal marker Brachury (*red*) and endodermal marker FOXA2 (green) in BMP4 + FGF2 induced mesendoderm differentiation of WT and *Cnot3*-DM ESCs for 4 days in the presence of combinations of Activin A, CHIR99021 and Wnt3 (as

32

indicated). Merged images show the mesendodermal cells. Nuclei were stained with DAPI; scale bar: 100 μm.

**Figure 4: CNOT3-T292/S294 phosphorylation promotes survival of differentiating mesendodermal cells. A.** Top panel: Crystal violet staining showing the efficiency of BMP4 + FGF2 induced mesendoderm differentiation of WT and *Cnot3*-DM ESCs after 4 and 8 days. Bottom panel: At the indicated time-points, live cells were counted based on trypan blue exclusion. X-axis = percentage of live cells at different time points of differentiation. Mean ± SEM; unpaired *t*-test between WT and CNOT3-DM for each time-point ***P<0.001 *n*=3. Crystal violet staining of two other clones of *Cnot3*-DM ESCs is shown in Figure S3A. **B.** Representative phase-contrast images showing the efficiency of BMP4 + FGF2 induced mesendoderm differentiation of WT and *Cnot3*-DM ESCs for 2, 4, and 8 days. Scale bar: 100 μm. See also Supplementary Video 1 for a time-lapse analysis of the differentiations. **C-E.** Representative IF analyses of images of staining for mesodermal marker Brachury (*red*) and endodermal marker FOXA2 (green) (**C**) or SMA (green) (**D**) and GATA4 (**E**) carried out on BMP4 + FGF2 induced mesendoderm differentiation of WT and *Cnot3*-DM ESCs for 4 days (*left panel;* scale bar:100 μm). Merged images show the mesendodermal cells. (D: scale bar = 60 μm). Nuclei were stained with DAPI. For IF analysis at 8 days of differentiation, see also Figures S3C and Figure S3D. **E.** IF analysis images of apoptotic markers Annexin V(*green*) and PI (red), in BMP4 + FGF2 induced mesendoderm differentiation of WT and *Cnot3*-DM ESCs for 4 days. Merged images show the Annexin V and PI stained apoptotic cells. Nuclei were stained with DAPI; scale bar: 100 μm. Histogram represents ratio of apoptotic cells to

33

total number of cells. Apoptotic cells were counted from ten randomly chosen fields for each biological replicate. Mean ± SEM; *t*-test **P<0.01 *n*=3.

**Figure 5: The CNOT3-T292A/S294A double mutation reduces ERK phosphorylation during mesendodermal differentiation. A.** Phase-contrast images showing the effects of MEK inhibitors that abolish ERK activity (PD0325091 and U0126) and FGFR inhibitor AZD4547 on BMP4 + FGF2 induced mesendoderm differentiation of WT and *Cnot3*-DM ESCs for 4 days. Each inhibitor was added after two days of differentiation. Scale bar: 100 μm. **B.** Immunoblotting analysis of the indicated proteins from the cell extracts prepared from BMP4 + FGF2 induced mesendoderm differentiation of WT and *Cnot3*-DM ESCs for 4 days. Loading control: α-Tubulin. **C.** Immunoblotting analysis of the indicated proteins from BMP4 + FGF2 induced mesendoderm differentiation of WT and *Cnot3-DM* ESCs carried out for 4 days, and treated with Aurora B inhibitor AZD1152 and MEK inhibitor PD0325091 for 5 hours and 10 hours respectively before harvesting. Loading control: α-Tubulin. **D.** Immunoblotting analysis of the indicated proteins from the cell extracts prepared from BMP4 + FGF2 induced mesendoderm differentiation of WT and *Cnot3*-DM ESCs for 4 days, following IP carried out with anti-CNOT3 antibody. Negative control: rabbit IgG. Input = 5% of extracts.

**Figure 6: Phosphorylation of CNOT3-T292/S294 regulates expression of genes that are involved in cell survival and proliferation. A.** Volcano plot of RNA-Seq transcriptome data showing differentially expressed genes after 4 days of BMP4 + FGF2 induced mesendoderm differentiation of WT and *Cnot3*-DM

ESCs. Fold change ratio >1.5; adjusted P value <0.05. Three biological replicates for each were analyzed. **B.** Principal component plot of the RNA-seq data showing PC1 and PC2 and the percent variance obtained for each. This reveals separate clustering of the genes that are differentially expressed between the WT and *Cnot3*-DM-derived 4-day differentiated mesendodermal cells. **C. and D.** Gene ontology analysis depicting upregulated genes (**C**) and downregulated genes (**D**) that are involved in signalling pathways that have key roles in developmental processes. Adjusted P value <0.05. **E.** GSEA analysis depicting Hallmark gene sets that were significantly altered in the differentiated cells. Fold change ratio >1.5; adjusted P value <0.05.

**Figure 7: Phosphorylation of CNOT3-T292/S294 alters interaction of CNOT3 with Aurora B and ERK in mesendodermal cells.** PLA detection of endogenous interaction between Aurora B and CNOT3 (**A**) and CNOT3 and ERK (**B**) in the BMP4 + FGF2 induced 4-day differentiated mesendoderm cells from WT and *Cnot3*-DM ESCs. Red dots represent positive PLA signals. Nuclei were stained with DAPI and cytoplasm with anti-tubulin. Boxed areas represent an enlarged cell indicated by the arrows; scale bar: 100 μm. PLA dots were quantified from randomly chosen fields from at least 50 cells for each biological replicate. Histograms represent average interactions per cell (dots/cell) as well as the nuclear (blue) and cytoplasmic (green) levels. Mean ± SEM; unpaired *t*-test ***P<0.001 (**A**) *n*=3 (**B**) *n*=2. Single antibody controls and PLA of CNOT3 and ERK using a second set of antibodies are shown in Figure S5.
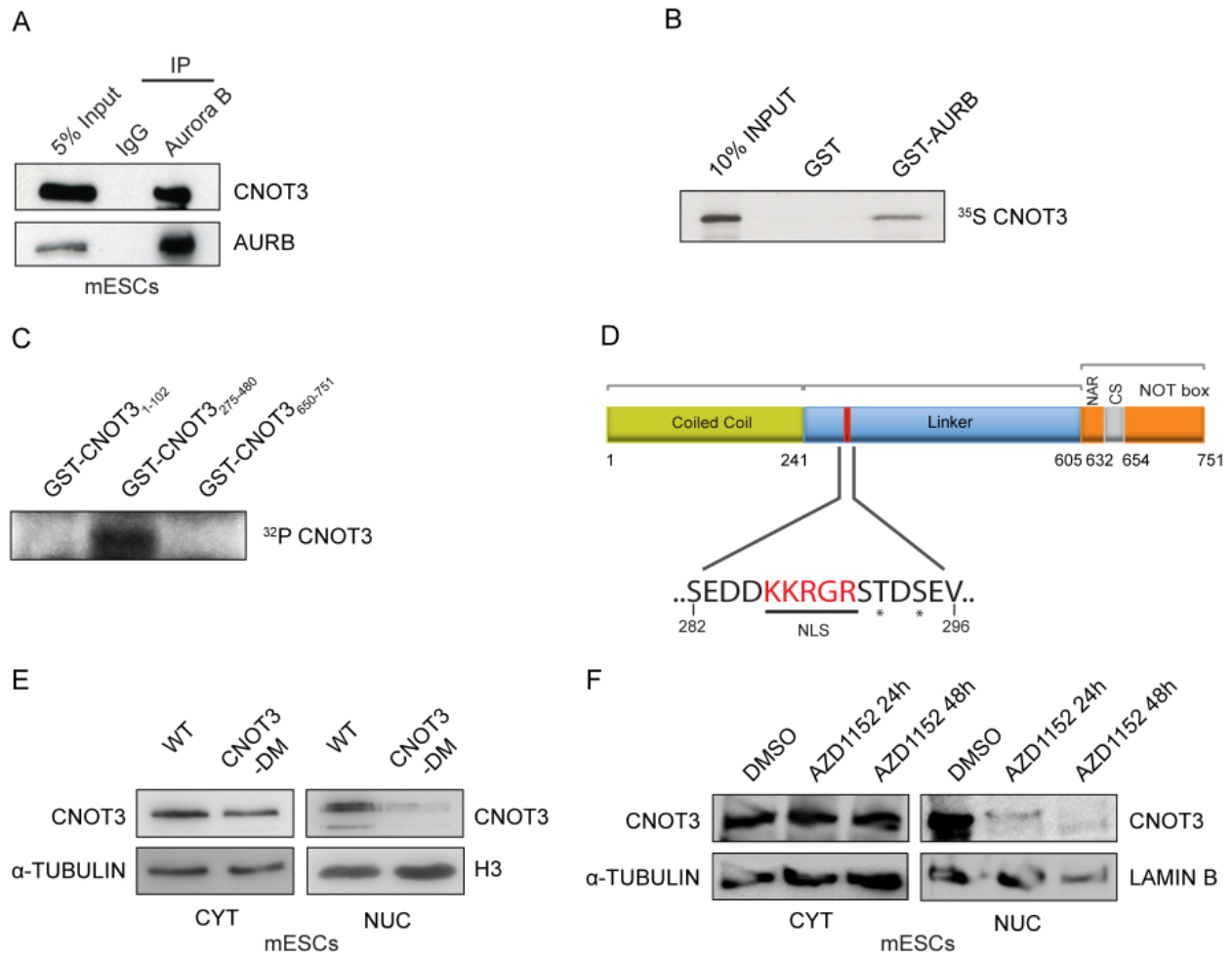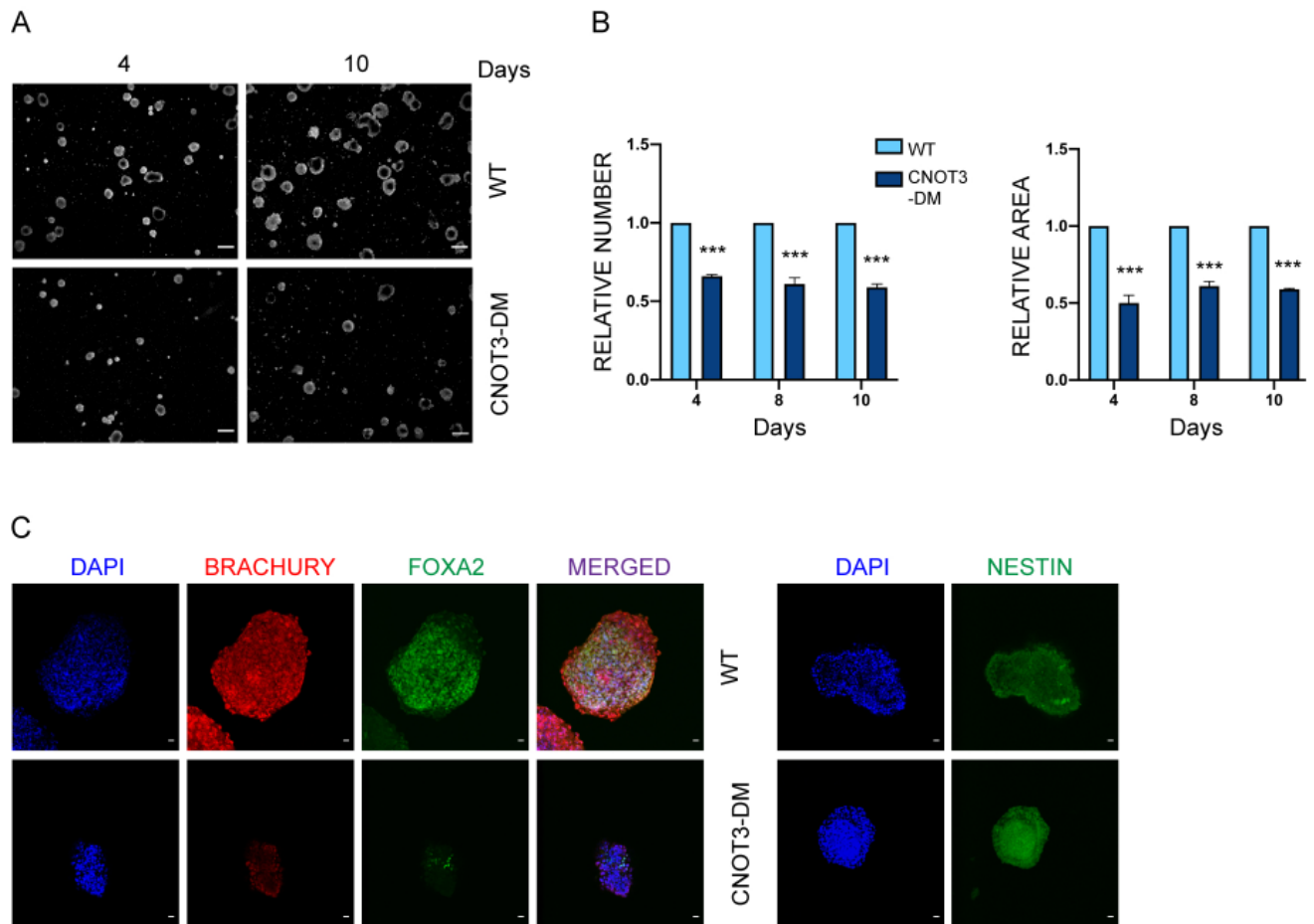
## FIGURE 1

# FIGURE 2


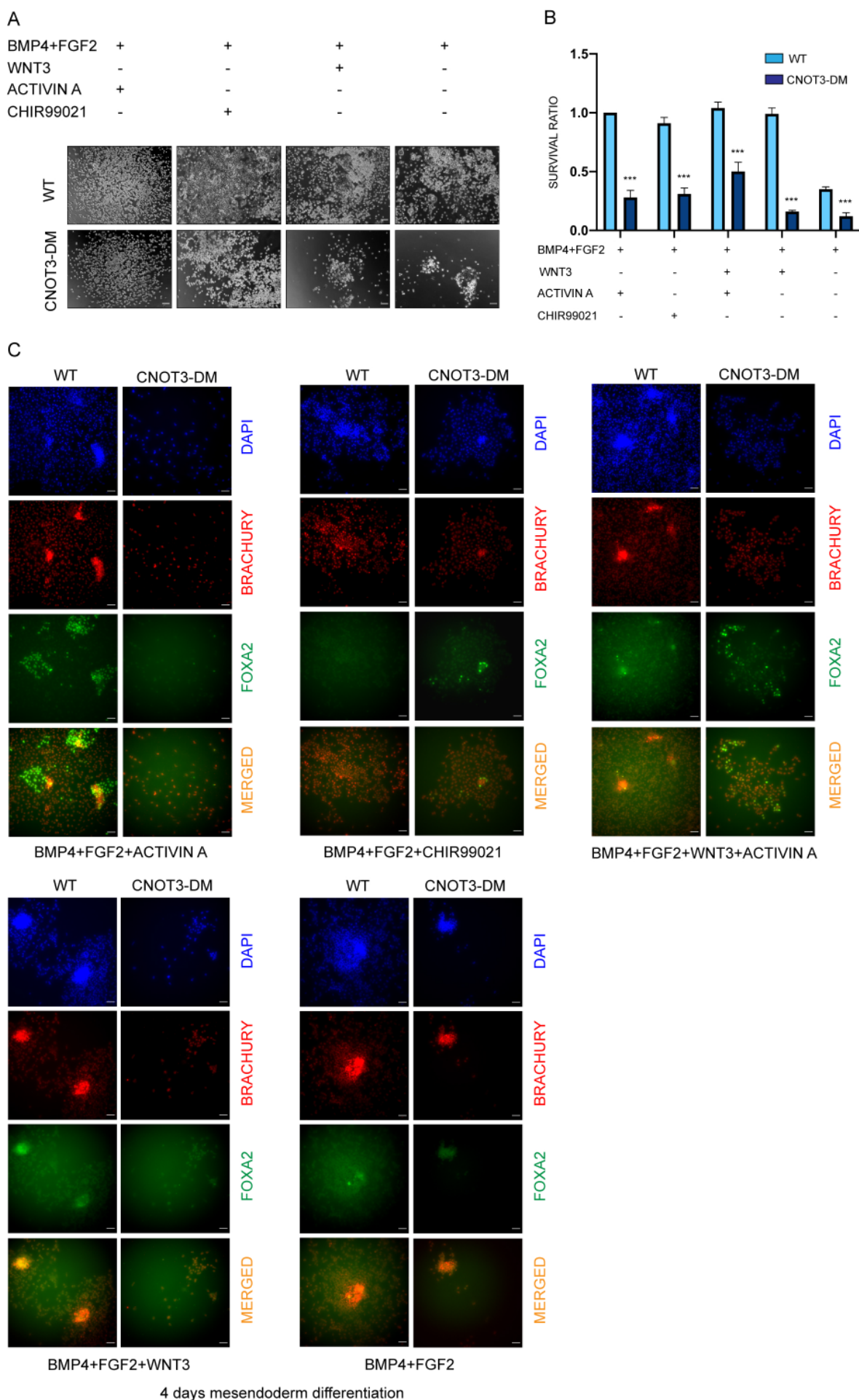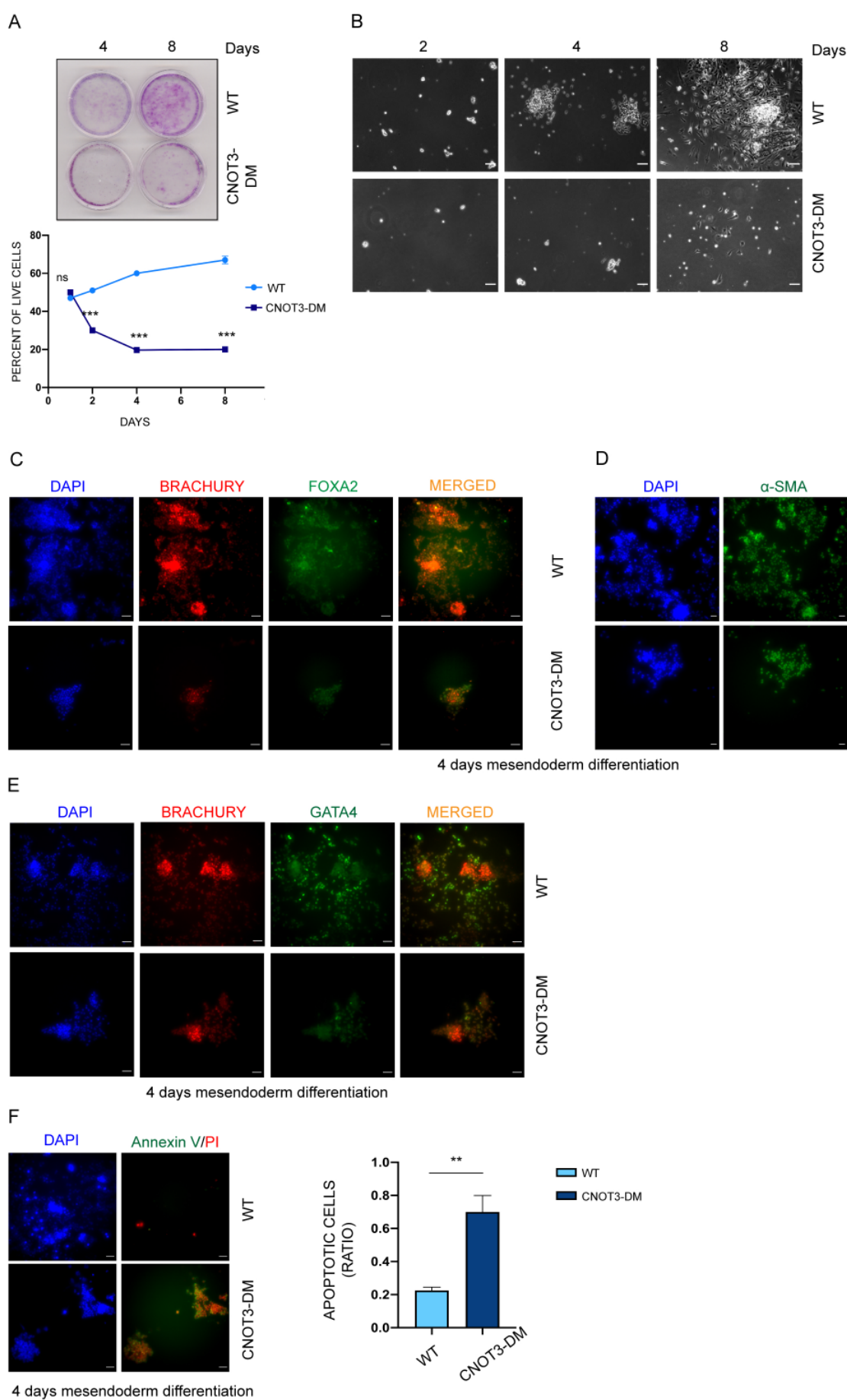
37

# FIGURE 3

## A

| | | | | |
|---|---|---|---|---|
| BMP4+FGF2 | + | + | + | + |
| WNT3 | - | - | + | - |
| ACTIVIN A | + | - | - | - |
| CHIR99021 | - | + | - | - |



## B



| | | | | | |
|---|---|---|---|---|---|
| BMP4+FGF2 | + | + | + | + | + |
| WNT3 | - | - | + | + | - |
| ACTIVIN A | + | - | + | - | - |
| CHIR99021 | - | + | - | - | - |

## C



BMP4+FGF2+ACTIVIN A



BMP4+FGF2+CHIR99021



BMP4+FGF2+WNT3+ACTIVIN A



BMP4+FGF2+WNT3



BMP4+FGF2

4 days mesendoderm differentiation

FIGURE 4



4 days mesendoderm differentiation

4 days mesendoderm differentiation

4 days mesendoderm differentiation

39

## FIGURE 5



A

BMP4+FGF2

DMSO    PD0325091    U0126    AZD4547    4 days

CNOT3-DM

B

CNOT3
P-ERK T202/Y204
ERK1/2
α-TUBULIN

4-day mesendoderm
differentiated cells

C

P-ERK T202/Y204
ERK1/2
α-TUBULIN

4-day mesendoderm
differentiated cells

D

5% Input    IP:CNOT3

CNOT3
AURB

4-day mesendoderm
differentiated cells

FIGURE 6



41

## FIGURE 7